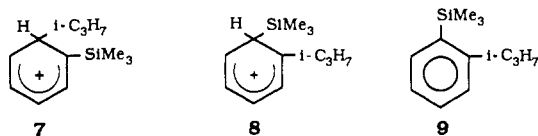faithfully reproduces the initial orientation.

Two experimental features are salient: First, even at Et_3N pressures in the range of 5–10 Torr, which entirely suppress protodesilylation, alkyldesilylation still occurs with a relative yield of ca. 20%. In the same systems, the isomeric composition of the products is characterized by a remarkably low extent (2%) of substitution ortho to the $SiMe_3$ group.

There are several ways to account for the inability of Et_3N to prevent alkyldesilylation as efficiently as protodesilylation. A first explanation can be based on the occurrence of direct ipso substitution. Whereas direct protonation of the ring position bearing the $SiMe_3$ group yields ion 6, whose reaction with Et_3N does not lead to desilylation, direct ipso isopropylation (eq 1b) gives instead ion 2, which can only be desilylated by Et_3N, yielding cumene. According to this view, the fraction of alkyldesilylation that cannot be suppressed by Et_3N reflects the extent of ipso alkylation of TSB.

Independent evidence for the role of ipso alkylation is provided by the significant proportions (20–27%) of p-cymene from the isopropylation of p-TST in the presence of Et_3N, although it could be argued that the methyl group of p-TST specifically activates the carbon bearing the $SiMe_3$ group.

An alternative explanation proceeds from the remarkably low extent of isopropylation ortho to the $SiMe_3$ group of TSB, which cannot be traced to steric hindrance to the $i\text{-}C_3H_7^+$ attack, since other gaseous cations of comparable size, such as $(CH_3)_2F^+$ and $CH_3O^+(H)NO_2$, give significant proportions of ortho-substituted isomers, respectively, 18% (Table II) and 37%.[21] Steric factors could instead hinder the subsequent deprotonation of the arenium ion 8 formed via a fast, energetically favored[13] proton 1,2-shift

from the primary adduct 7. The steric compression arising from the coplanarity of the $SiMe_3$ and of the $i\text{-}C_3H_7$ substituent in the deprotonated product 9 could affect the selectivity in the Et_3N reaction in favor of desilylation, inverting the bias in favor of deprotonation noted in the sterically unhindered arenium ion 6.[22]

Such interpretation takes into account the ability of Et_3N to bind to $SiMe_3^+$, demonstrated by ICR spectrometry,[13] and has the advantage of accounting both for the failure of Et_3N to suppress alkyldesilylation as efficiently as protodesilylation and for the remarkably low extent of substitution ortho to the $SiMe_3$ group, a feature noted as well in the alkylation of p-TST. In this connection, we note that steric hindrance to deprotonation has previously been reported in the gas-phase isopropylation of crowded arenes.[23]

A clear–cut decision between the explanations outlined above of the failure of Et_3N to entirely suppress alkyldesilylation cannot at present be made, especially since they are not mutually exclusive. It can only be asserted with a sufficient degree of confidence that the desilylated products still detectable in the presence of 5–10 Torr of Et_3N arise from the direct attack on the carbon bearing the $SiMe_3$ group and/or from the alkylation of the ortho positions. It follows that the combined extent of ipso and ortho substitution of TSB by $i\text{-}C_3H_7^+$ should amount to ca. 20%.

7   8   9

(21) Attinà, M.; Cacace, F.; Ricci, A. Gazz. Chim. Ital. 1989, 119, 217.

(22) The postulated dependence of the deprotonation/desilylation branching ratio in the Et_3N reactivity on the nature of the arenium ion is not unprecedented, e.g., there is evidence that $Me_2N(CH_2)_2OH$, which acts exclusively as a desilylating reagent toward 6, see refs 11 and 12, can deprotonate, as well as desilylate, ions 3.

(23) Aliprandi, B.; Cacace, F.; Cipollini, R. Radiochim. Acta 1982, 32, 1072.

Gas-Phase Proton-Transfer Reactions between Alkoxide Anions

James A. Dodd, Susan Baer, Christopher R. Moylan, and John I. Brauman*

Contribution from the Department of Chemistry, Stanford University, Stanford, California 94305-5080. Received September 10, 1990

Abstract: Reaction efficiencies for proton transfer between alkoxide anions and neutral alcohols have been measured in an ion cyclotron resonance spectrometer, using a competition kinetics technique. The efficiencies for identity proton-transfer reactions are measurably less than 0.5, which is the simple statistical prediction for a thermoneutral reaction with no energetic barrier. In addition, the trend in reaction efficiencies for exothermic proton transfers is consistent with the presence of a substantial Marcus intrinsic barrier. An energetic barrier of this magnitude is not consistent with a surface which is believed to have little or no barrier. The results are consistent, however, with recent quasi-classical trajectory calculations which show that efficiencies for reactions on a barrierless surface can be slower than expected.

I. Introduction

While sophisticated equilibrium studies have significantly enhanced our understanding of the thermodynamics that govern gas-phase proton-transfer reactions,[1] the corresponding kinetics are less well characterized. Certain characteristics are known to decrease reaction rates, including charge delocalization and steric hindrance.[2] For example, gas-phase proton transfers involving delocalized carbanions are often slow, occurring on only a small fraction of ion–molecule collisions.[2a,b] These rate decreases have been attributed to considerable energetic barriers on the potential

(1) For example, see: (a) McMahon, T. B.; Kebarle, P. J. Am. Chem. Soc. 1985, 107, 2612. (b) Larson, J. W.; McMahon, T. B. J. Phys. Chem. 1984, 88, 1083. (c) Larson, J. W.; McMahon, T. B. J. Am. Chem. Soc. 1984, 106, 517. (d) Larson, J. W.; McMahon, T. B. J. Am. Chem. Soc. 1983, 105, 2944. (e) Yamdagni, R.; Kebarle, P. J. Am. Chem. Soc. 1971, 93, 7139. (f) Caldwell, G.; Rozeboom, M. D.; Kiplinger, J. P.; Bartmess, J. E. J. Am. Chem. Soc. 1984, 106, 4660.

(2) (a) Han, C.-C.; Brauman, J. I. J. Am. Chem. Soc. 1989, 111, 6491. (b) Meyer, F. K.; Pellerite, M. J.; Brauman, J. I. Helv. Chim. Acta 1981, 64, 1058. (c) Farneth, W. E.; Brauman, J. I. J. Am. Chem. Soc. 1976, 98, 7891. (d) Lias, S. G.; Shold, D. M.; Ausloos, P. J. Am. Chem. Soc. 1980, 102, 2540. (e) Jasinski, J. M.; Brauman, J. I. J. Am. Chem. Soc. 1980, 102, 2906. (f) Meot-Ner, M. J. Am. Chem. Soc. 1982, 104, 5. (g) Rakshit, A. B.; Warneck, P. J. Chem. Phys. 1981, 74, 2853.

Gas-Phase Proton Transfer between Alkoxide Anions

J. Am. Chem. Soc., Vol. 113, No. 16, 1991 5943

energy surface. In some cases, however, other types of bottlenecks have been suggested.[3a,b] In hydride-transfer reactions, for example, slow rates have been attributed to entropic bottlenecks on a barrierless potential energy surface.[3c,d] Kebarle and co-workers have ascribed these bottlenecks to the loss of rotations engendered by the approach of the two reactants.[3c]

Simple proton-transfer reactions between anions with localized charge are not expected to have large energetic barriers. In solution, the majority of exothermic proton-transfer reactions between alkoxide ions occur at the diffusion limit.[4] Proton transfer between water and hydroxide in the gas phase has been extensively studied[5,6] and found to be fast. Results pertaining to proton transfer between gas-phase alkoxides, however, have been more ambiguous, in part because of uncertainties in estimating the absolute collision rate constant. Although early experiments by Bohme et al.[7] and Lieder[8a] suggested that these reactions were fast, more recent, sensitive rate measurements suggest that the reactions are subtly slowed relative to the collision rate constant.[8b] Work by DePuy, Bierbaum, and co-workers[6,9] appeared initially to support collision-controlled rates, but more recent work indicates that exchange between labeled methoxide anions is up to 20% slower than the collision rate.

In this paper, we report an extensive study of alkoxide ion proton-transfer reaction rates; our results indicate that not only are thermoneutral proton exchanges measurably slow, but reactions up to 6 kcal/mol exothermic are still less than unit efficient. We do not believe these slow reaction rates can be explained by insufficiently thermalized ions because the rate constants measured at high pressure (where the ions are certainly thermalized) show similar behavior.[6,9] These surprising results suggest that the potential energy surface must possess some type of energetic or dynamic barrier.

Section II gives experimental information and presents a competitive reaction technique which was used to measure the reaction rate constants, thereby minimizing the inherent error in pressure measurements and the uncertainty in the collision rate constant. The kinetic results are presented in section III.

Important information about proton-transfer reactions can be obtained by ab initio studies of the potential energy surface. In section IV, we present a review of pertinent quantum calculations and discuss the implications for the reaction kinetics. An analysis of the kinetic results in terms of a statistical model is presented in section V, followed by a general discussion in section VI. The statistical model is shown to give a result that is inconsistent with the quantum calculations. We conclude that the slowing of these reactions is not a consequence of an energetic barrier and that use of a *simple* RRKM model is inappropriate for these reactions.

II. Experimental Section

Reagents. All chemicals were purchased from Aldrich and were used as received with the exception of the compounds specifically mentioned

Scheme I
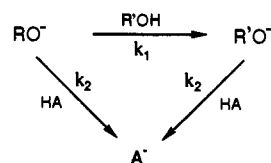
below. Samples were degassed using three freeze–pump–thaw cycles prior to introduction to the high-vacuum system. Dimethyl and diethyl peroxide were prepared using adaptations of literature recipes.[10] Methyl nitrite and ethyl nitrite were synthesized in situ by reaction of isoamyl nitrite and the appropriate alcohol.[11] Isotopically labeled alcohols were purchased from MSD Isotopes.

Experimental System. All the experiments utilized ion cyclotron resonance (ICR) spectrometry, which has been described in detail elsewhere.[12] The kinetic measurements were performed successively over a period of several years during which the system was switched from a single-ion detection scheme to a Fourier transform ion cyclotron resonance spectrometer (Ion Spec FTMS 2000), which enables one to excite and detect all ions simultaneously.[13] This modification facilitates the experiment enormously; all ion processes can be observed simultaneously, the signal/noise ratio is improved, and faster speeds allow more averaging. This modification was not found to affect the experimental results. Experiments were performed in a 1-in. cubic cell placed between the poles of an electromagnet, which was operated at 1.0–1.2 T. Typical background pressures were 0.5–2 × 10^{-8} Torr.

Neutral gas pressures were measured using a Varian 844 vacuum ionization gauge, which was calibrated daily for each gas, using an MKS Baratron manometer. The Baratron itself was calibrated by MKS; its accuracy was checked periodically by measuring the rate constant of eq 1, a reaction for which the rate constant, 1.1 × 10^{-9} cm^3 molecule^{-1} s^{-1}, is known with good accuracy.[14]

$$CH_4 + CH_4^+ \rightarrow CH_3 + CH_5^+ \qquad (1)$$
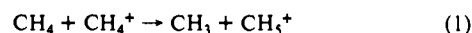
The experiments were performed at low pressures; typically, 1–2 × 10^{-7} Torr of the primary ion source and 2–8 × 10^{-7} Torr of the neutral reactant were used. Methoxide, ethoxide, and *tert*-butoxide were generated by electron impact on their corresponding peroxides. Labeled alkoxides, CD$_3$O$^-$ and CD$_3$CH$_2$O$^-$, were generated by electron impact on CD$_3$ONO and CD$_3$CH$_2$ONO, respectively.[11] Hydroxide was generated by electron impact on N$_2$O to yield O$^-$, which subsequently reacted with butane via hydrogen atom abstraction. In this case, it was necessary to introduce 4 × 10^{-6} Torr of a 1:5 N$_2$O/butane mixture in order to generate an acceptable ion signal.

Kinetic Measurements. Kinetic rate measurements in these low-pressure regimes have rather large uncertainties due to the difficulty of absolute pressure measurements in this region. As described above, all precautions were taken to minimize the uncertainties in the pressure measurements, but the reliability in the absolute rate constants remains ≈±25%. In addition, uncertainty in the collision rate constant also contributes to error in the reported reaction efficiency. Recent advances in collision rate theory have improved estimates of the collision rate constant,[15-21] but discrepancies remain.[9,21,22]

(3) (a) Bowers, M. T.; Jarrold, M. F.; Wagner-Redeker, W.; Kemper, P. R.; Bass, L. M. *Faraday Discuss. Chem. Soc.* **1983**, *75*, 57. (b) Bowers, M. T.; Chesnavich, W. J. *Prog. React. Kinet.* **1982**, *11*, 137. (c) Sunner, J. A.; Hirao, K.; Kebarle, P. *J. Phys. Chem.* **1989**, *93*, 4010. (d) Magnera, T. F.; Kebarle, P. In *Ionic Processes in the Gas Phase*; Almoster-Ferreira, M. A., Ed.; D. Reidel Publishing: Dordrecht, Holland, 1984; p 135.

(4) (a) Crooks, J. E. In *Proton Transfer Reactions*; Caldin, E. F., Gold, V., Eds.; Wiley: New York, 1975; Chapter 6. (b) Caldin, E. F. *Fast Reactions in Solution*; Wiley: New York, 1964; Chapters 1 and 12. (c) Bell, R. P. *The Proton in Chemistry*; Cornell University Press: Ithaca, New York, 1959.

(5) (a) Grabowski, J. J.; DePuy, C. H.; Bierbaum, V. M. *J. Am. Chem. Soc.* **1983**, *105*, 2565. (b) Meot-Ner, M.; Lloyd, J. R.; Hunter, E. P.; Agosta, W. A.; Field, F. H. *J. Am. Chem. Soc.* **1980**, *102*, 4672.

(6) Grabowski, J. J.; DePuy, C. H.; Van Doren, J. M.; Bierbaum, V. M. *J. Am. Chem. Soc.* **1985**, *107*, 7384. The efficiences reported here would be lower if the Su–Chesnavich collision rate constant had been used.

(7) Bohme, D. K.; Lee-Ruff, E.; Young, L. B. *J. Am. Chem. Soc.* **1972**, *94*, 5153.

(8) (a) Lieder, C. A. Ph.D. Thesis, Stanford University, 1974; p 192. (b) Moylar, C. R.; Jasiaski, J. M.; Brauman, J. I. *J. Am. Chem. Soc.* **1985**, *107*, 1934.

(9) Barlow, S. E.; Dang, T. T.; Bierbaum, V. M. *J. Am. Chem. Soc.* **1990**, *112*, 6832.

(10) (a) Dimethyl peroxide: Hanst, P. L.; Calvert, J. G. *J. Phys. Chem.* **1959**, *63*, 104. (b) Diethyl peroxide: Harris, E. J.; Egerton, A. C. *Proc. R. Soc. London* **1938**, *A168*, 1.

(11) Caldwell, G.; Bartmess, J. E. *Org. Mass Spectrom.* **1982**, *17*, 19.

(12) (a) McIver, R. T., Jr. *Rev. Sci. Instrum.* **1978**, *49*, 111. (b) McIver, R. T., Jr.; Hunter, R. L.; Ledford, E. B., Jr.; Locke, M. J.; Francl, T. J. *Int. J. Mass. Spectrom. Ion Phys.* **1981**, *39*, 65.

(13) For a recent review of this technique, see: Freiser, B. S. In *Techniques for the Study of Ion-Molecule Reactions*; Farrar, J. M., Saunders, W. H., Jr., Eds.; John Wiley: New York, 1988; Chapter 3.

(14) (a) Su, T.; Bowers, M. T. *Int. J. Mass Spectrom. Ion Phys.* **1973**, *12*, 347. (b) Su, T.; Bowers, M. T. *J. Chem. Phys.* **1973**, *58*, 3027.

(15) (a) Bates, D. R. *Proc. R. Soc. London* **1984**, *384*, 289. (b) Bates, D. R. *Chem. Phys. Lett.* **1981**, *82*, 396.

(16) Su, T.; Chesnavich, W. J. *J. Chem. Phys.* **1982**, *76*, 5183.

(17) Chesnavich, W. J.; Su, T.; Bowers, M. T. *J. Chem. Phys.* **1980**, *72*, 2641.

(18) (a) Clary, D. C.; Smith, D.; Adams, N. G. *Chem. Phys. Lett.* **1985**, *119*, 320. (b) Clary, D. C. *Mol. Phys.* **1985**, *54*, 605.

(19) Troe, J. *J. Chem. Phys.* **1987**, *87*, 2773.

(20) Markovic, N.; Nordholm, S. *Chem. Phys.* **1989**, *135*, 109.

(21) (a) Su, T. *J. Chem. Phys.* **1988**, *88*, 4102. (b) Su, T. *J. Chem. Phys.* **1988**, *89*, 5355.

(22) (a) Swamy, K. N.; Hase, W. L. *J. Chem. Phys.* **1982**, *77*, 3011. (b) Swamy, K. N.; Hase, W. L. *J. Am. Chem. Soc.* **1984**, *106*, 4071.

Table I. Efficiencies for Proton-Transfer Reactions

reaction	efficiency[a]	efficiency[b]	$\Delta E_{rxn}^{\circ\,c,d}$
(1) $HO^- + D_2O$	0.42	0.44 (4)	+0.3[e]
(2) $CH_3O^- + {}^{13}CH_3OH$		0.26 (1)	0.0
(3) $CH_3O^- + CD_3OH$	0.18	0.20 (4)	+0.5[f]
(4) $CD_3O^- + CH_3OH$		0.35 (3)	−0.5[f]
(5) $C_2H_5O^- + CD_3CH_2OH$		0.30 (1)	0.0
(6) $C_2H_5O^- + C_2D_5OD$		0.15 (1)	≥0
(7) $t\text{-}C_4H_9CO^- + t\text{-}C_4D_9COD$	0.28	0.23 (2)	≥0
(8) $CH_3O^- + C_2H_5OH$		0.41 (5)	−3.1
(9) $CH_3O^- + t\text{-}C_4H_9OH$	0.51	0.57 (4)	−5.9
(10) $CH_3O^- + CF_3CH_2OH$		0.85 (3)	−14.8
(11) $CH_3O^- + PhOH$	1.07		−27.8
(12) $t\text{-}C_4H_9O^- + PhOH$	1.03		−21.9

[a] Efficiency calculated using $k/k_{\text{Su–Chesnavich}}$.[16] [b] Efficiency calculated using competition kinetics and eq 2. The numbers in parentheses are one standard deviation (in the last significant figure) over the experimental determinations. [c] Energies are given in kcal/mol. [d] Reference 32. [e] Reference 34. [f] Reference 33.

In order to minimize the sources of error listed above and provide the most sensitive possible rate measurement, a kinetic competition technique was developed. Instead of monitoring the pseudo-first-order decay of the alkoxide ion as it reacts with the neutral alcohol, this technique measures the relative yield of the proton-transfer product ion versus the product ion for a reaction that we assume to occur on every collision. For proton-transfer reactions, a strong acid, HA, that will quickly donate a proton is chosen. In this way, the important parameters are the relative pressure of the neutral alcohol versus HA and the relative collision frequencies for the alcohol and the reference acid. Using this technique, the error in the reaction efficiencies is estimated to be ±15%.

The processes involved in this technique are shown in Scheme I. The cell contains the appropriate alkyl peroxide, ROOR, or alkyl nitrite, RONO; the reacting alcohol, R′OH; and the reference acid, HA, usually phenol. Electron impact produces RO^- which undergoes proton transfer with the neutral acids R′OH and HA in the cell. The reaction is first allowed to go to completion, i.e., to the point when only A^- is present in the cell, and the intensity of the A^- signal is measured. Second, a continuous oscillating frequency is applied to $R'O^-$ to eject it from the cell as soon as it is formed. The intensity of the A^- signal is decreased because the contribution from $R'O^-$ has been eliminated. The signal with RO'^- ejection is proportional to the primary A^- yield; the difference between the two signals is proportional to the $R'O^-$ yield. The relative primary yields of $R'O^-$ and A^-, determined in this way, can be substituted into eq 2 to determine the reaction efficiency. In this equation, the

$$\text{efficiency} = \frac{[R'O^-]_1}{[A^-]_1} \frac{P_{HA}}{P_{ROH}} \frac{k_{c,HA}}{k_{c,ROH}} \qquad (2)$$

subscript "1" denotes primary yield, P_{HA} and P_{ROH} are the neutral gas pressures of HA and ROH, respectively, and k_c is the appropriate collision rate constant, calculated using the method of Su and Chesnavich[17] at 350 K, the estimated temperature of the ICR cell.[23]

Reactions involving ethoxide anion presented some difficulties, since both methods of generation (diethyl peroxide or ethyl nitrite) also create side reactions. When diethyl peroxide was used, its pyrolysis on the filament gave acetaldehyde which reacted with EtO^- to give $C_2H_3O^-$. In the nitrite method, NO_2^- was generated by reaction of EtO^- with ethyl nitrite. Thus in both cases, a third channel for disappearance of the primary ion is available. The peroxide method is further complicated by the subsequent reaction of $C_2H_3O^-$ to generate A^-, whereas the NO_2^- formed in the nitrate method does not undergo further reactions. The appropriate ratio, $[EtO^-]/[A^-]$, can be obtained in both cases, but the kinetic analysis is slightly more complicated. These derivations and a more formal analysis of the simple case, with no side reactions, are presented in Appendix A.

Phenol was the primary reference acid used in this study. Trifluoroethanol was also used in the reaction of hydroxide plus water. A few rates were also measured with hydrogen sulfide as a reference acid. Measured reaction rates were found to be independent of the acid used.

III. Results

The reaction efficiencies measured in this work using the competition method outlined in the Experimental Section are listed in Table I. For comparison, selected efficiencies were measured using the traditional technique of monitoring pseudo-first-order

decay of reactant ion. These results are also included in the table. The uncertainties in the efficiencies arising from the competition experiments are one standard deviation over the three to four experiments performed for each efficiency listed. These range from 0 to 15% of the efficiency, and the error can be conservatively estimated at ±15%. The error in the traditional measurements is estimated at ±25%.

The standard enthalpies of reaction are also given in Table I.[24-26] The enthalpies for reactions 6 and 7 are unknown. They are expected to be slightly endothermic, however, since most equilibrium isotope effect studies suggest that the stretching motion involving the isotope has a larger force constant in the neutral species than in the ion.[27] More specifically, delocalization of the negative charge into the antibonding C–H orbitals lowers the force constants in the negative ion.[27a] Thus, deuterium-substituted compounds are generally weaker acids.

As can be seen from Table I, the reaction efficiencies obtained for the two thermoneutral reactions, (2) and (5), are considerably less than 50%. The measured efficiency of 26% for reaction of methoxide with ${}^{13}C$-labeled methanol is in rough agreement with the efficiency measured by Bierbaum and co-workers.[9] The efficiency measured for ethoxide + CD_3CH_2OH, 30%, is also consistent with both of these numbers. The endothermic reaction, (3), is further slowed, as would be expected; the reaction efficiency is 20%. The efficiencies for the (presumably) endothermic reactions, (6) and (7), are 15% and 23%, respectively.

Perhaps most surprisingly, the exothermic reactions 4, 8, 9, and 10 are also slow. Deuterated methoxide + methanol, reaction 4, is 0.5 kcal/mol exothermic and its efficiency is still less than 50%, as is methoxide + ethanol, (8), which is 3 kcal/mol exothermic. Reaction of methoxide + *tert*-butyl alcohol, (9), is almost 6 kcal/mol exothermic and still shows an efficiency of less than one. Even the strongly exothermic reaction of methoxide with trifluoroethanol ($\Delta H^\circ = -14.8$ kcal/mol) is less than unit efficient.

The reaction rate of hydroxide with deuterated water, reaction 1 in Table I, is expected to differ from 50% due to several factors. First, the reaction is slightly endothermic ($\Delta H^\circ = +0.3$ kcal/mol), resulting in a decreased efficiency. Second, since either deuterium can be abstracted from D_2O, symmetry factors must be included. Including both these factors, the deuterium-transfer reaction would be expected to have a reaction efficiency of 55% for a barrierless reaction surface. We find a reaction efficiency of 46% for hydroxide plus D_2O. This rate constant, 1.3×10^{-9} cm³ molecule⁻¹ s⁻¹, is in good agreement with a flowing afterglow measurement by DePuy et al.[5a] This result is also not inconsistent with rate constants by Field and co-workers, reported for an isotopically related reaction:

$$DO^- + H_2O \rightarrow OH^- + HDO \qquad \Delta H^\circ = -0.3 \text{ kcal/mol} \qquad (3)$$

These workers measured rates of 1.5×10^{-9} cm³ molecule⁻¹ s⁻¹ and 1.2×10^{-9} cm³ molecule⁻¹ s⁻¹ at 480 K and 595 K, respectively.[5b]

IV. Review of Quantum Calculations

Before discussing the slow reaction efficiencies described in the Results section, it is instructive to look at what is already known

(23) Han, C.-C. Ph.D. Thesis, Stanford University, 1987.

(24) Lias, S. G.; Bartmess, J. E.; Liebman, J. F.; Holmes, J. L.; Levin, R. D.; Mallard, W. G. *J. Phys. Chem. Ref. Data* **1988**, 17.

(25) ΔH°_{rxn} for $CH_3O^- + CD_3OH$ and $CD_3O^- + CH_3OH$: DeFrees, D. J.; Bartmess, J. E.; Kim, J. K.; McIver, R. T., Jr.; Hehre, W. J. *J. Am. Chem. Soc.* **1977**, *77*, 6451.

(26) ΔH_{rxn} for $HO^- + D_2O$: (a) Schulz, P. D.; Mead, R. D.; Jones, P. L.; Lineberger, W. C. *J. Chem. Phys.* **1982**, *77*, 1153. (b) Shimanouchi, T. *Tables of Molecular Vibrational Frequencies*; Consolidated Vol. 1; Natl. Stand. Ref. Data Ser., National Bureau of Standards: Washington, D.C., 1972.

(27) (a) Wolfsberg, M. *Acc. Chem. Res.* **1972**, *5*, 225. (b) DeFrees, D. J.; Hassner, D. Z.; Hehre, W. J.; Peter, E. A.; Wolfsberg, M. *J. Am. Chem. Soc.* **1978**, *100*, 641. (c) DeFrees, D. J.; Taagepara, M.; Levi, B. A.; Pollack, S. K.; Summerhays, K. D.; Taft, R. W.; Wolfsberg, M.; Hehre, W. J. *J. Am. Chem. Soc.* **1979**, *101*, 5532. (d) Hout, R. F., Jr.; Wolfsberg, M.; Hehre, W. J. *J. Am. Chem. Soc.* **1980**, *102*, 3296. (e) Hout, R. F., Jr.; Levi, B. A.; Hehre, W. J. *J. Comput. Chem.* **1983**, *4*, 499.

Gas-Phase Proton Transfer between Alkoxide Anions

J. Am. Chem. Soc., Vol. 113, No. 16, 1991 5945

about proton-transfer potential surfaces from quantum calcula-tions. Ab initio calculations of negatively charged species are complicated by the diffuse nature of the anion. In order to calculate accurate energies, diffuse and polarizable orbitals must be included in the basis set, greatly increasing the time and cost of the calculation. In addition, calculations of proton-transfer reactions have indicated that electron correlation effects must be included in order to provide an accurate treatment.[28,29] These constraints have slowed the development of high level calculation for larger proton-transfer systems, but several good calculations of smaller reactions exist, including hydroxide + water and methoxide + methanol.

In 1976, Roos et al.[28a] performed a benchmark calculation of the hydroxide + water system. They compared the equilibrium geometry and the binding energy of the hydrogen-bonded complex using a self-consistent field (SCF) model and large-scale con-figuration interaction (CI) to model the effects of electron cor-relation. Their SCF calculations showed an asymmetric geometric minimum with a 1.4-kcal/mol proton-transfer barrier, and a 24.5-kcal/mol binding energy. Inclusion of electron correlation effects, using CI, changed these numbers dramatically: the minimum energy structure became much more symmetric, the barrier height dropped to 0.15 kcal/mol, and the binding energy increased to 28.15 kcal/mol. These results emphasized the im-portance and magnitude of the electron correlation effects in a reaction involving breakage of a covalent bond.

Scheiner and co-workers[29] were able to duplicate these results for hydroxide + water using up to a 6-311G** basis set and Møller–Plesset (MP) perturbation theory to model the electron correlation effects. Similar geometries and barrier heights were obtained, and the same dependence of these parameters on the electron correlation effects as observed. These researchers have also studied the effect of the hydrogen bond length on the potential surface.[30] They find, not surprisingly, that stretching the O–O bond length sharply increases the height of the proton-transfer barrier.

A series of anion–water complexes have been studied by Gao, Garner, and Jorgensen.[31] These workers performed a geometry optimization of the methoxide–water complex at the Hartree–Fock (HF)/6-31G(d) level and obtained a slightly asymmetric geometry (HO–H = 0.996 Å, CH$_3$O–H = 1.646 Å). The proton-transfer barrier height was not calculated. An earlier work by the same research group reports an optimized geometry for CH$_3$O$^-$·HOCH$_3$ at the 4-31G level.[32] This geometry is similar to that of meth-oxide–water, with the relevant O–H bond lengths equal to 1.512 Å and 1.025 Å.

The methoxide + methanol potential surface has also been studied by de la Vega[33] at the 4-31G level. He obtained a more symmetric structure (1.1 Å, 1.3 Å) with a less than 1 kcal/mol barrier to proton transfer at that geometry. Like Scheiner, he found that small changes in the O–O bond distances cause large barrier increases. In addition, de la Vega found that rotation of the methyl moiety also sharply increases the barrier height. He also addressed the possibility of proton tunneling and found that it should be very fast for a symmetric reaction.[33,34] Small dis-tortions to that symmetry, however, such as the methyl rotation mentioned above, quickly slow down the tunneling rate.
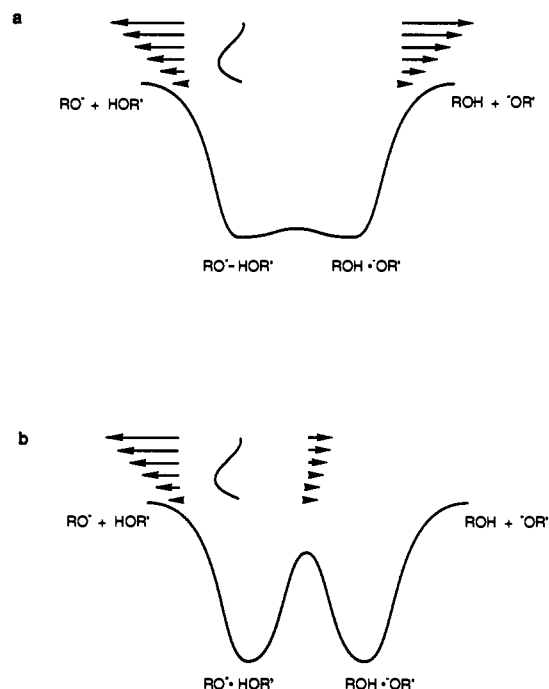

Figure 1. Schematic of branching behavior of RO$^-$·HOR' complexes for single and double minimum potentials (illustrated in a and b, respec-tively). The arrows signify the relative magnitude of the microcanonical rate constants for dissociation of the chemically activated alkoxide–al-cohol population.

Higher level calculations of the methoxide–methanol system have been performed by both Dixon[35] and Wolfe.[36] Dixon calculated an optimum geometry at the DZ+P level (OH bond lengths equal to 1.0 Å and 1.4 Å) and found a proton-transfer barrier height of 2.18 kcal/mol. Since this result does not include the effects of electron correlation, however, it must be regarded only as an upper limit. Wolfe obtained a similar geometry using a 6-31G(d)//6-31G(d) basis set; OH bond lengths equal to 1.0 Å and 1.55 Å. At this level, he obtained a barrier height of 2.91 kcal/mol. He also performed a four-point MP2/6-31+G(d) correction and found that the proton-transfer barrier decreases to less than 1 kcal/mol. A binding energy of 27.8 kcal/mol was reported.

These calculations of simple proton-transfer systems show im-pressive agreement on several important points. First, the binding energy of the complexes is ca. 25–30 kcal/mol. Second, the geometry of the minimum energy structure is asymmetric, and, third, there is an almost negligible barrier between the two minimum energy structures. These observations lead one to im-agine a quartic potential surface, with steep walls and a relatively flat bottom where the proton has an essentially unrestricted range of motion. Traditional statistical analysis and simple intuition point to a collision-controlled reaction rate for this type of min-imum energy pathway. For a thermoneutral reaction, this would yield a 50% reaction efficiency; the ion–molecule complex formed upon collision branches at equal rates into two identical exit channels, one of which regenerates reactants and one of which gives products.

Another interesting conclusion from these quantum calculations is that, although the minimum energy path has little or no barrier, any movement away from the optimum geometry sharply increases the barrier height. This implies, not unreasonably, that the tight transition state is more sensitive to distortions than the loose hydrogen-bonded complex. Thus, a three-dimensional picture of the surface shows a narrow trough surrounded by steeper and steeper pathways.

(28) (a) Roos, B. O.; Kraemer, W. P.; Diercksen, G. H. F. *Theor. Chim. Acta (Berlin)* **1976**, *42*, 77. (b) Støgard, A.; Strich, A.; Roos, B. *Chem. Phys.* **1975**, *8*, 405.

(29) (a) Scheiner, S.; Szczesniak, M. M.; Bigham, L. D. *Int. J. Quantum Chem.* **1983**, *23*, 739. (b) Szczesniak, M. M.; Scheiner, S. *J. Chem. Phys.* **1982**, *77*, 4586.

(30) (a) Scheiner, S. *Acc. Chem. Res.* **1985**, *18*, 174. (b) Scheiner, S.; Bigham, L. D. *J. Chem. Phys.* **1985**, *82*, 3316. (c) Scheiner, S. *J. Chem. Phys.* **1984**, *80*, 1982. (d) Hillenbrand, E. A.; Scheiner, S. *J. Am. Chem. Soc.* **1984**, *106*, 6266. (e) Scheiner, S. *J. Chem. Phys.* **1982**, *77*, 4039. (f) Scheiner, S. *J. Phys. Chem.* **1982**, *86*, 376. (g) Scheiner, S. *J. Am. Chem. Soc.* **1981**, *103*, 315.

(31) Gao, J.; Garner, D. S.; Jorgensen, W. L. *J. Am. Chem. Soc.* **1986**, *108*, 4784.

(32) Jorgensen, W. L.; Ibrahim, M. *J. Comput. Chem.* **1981**, *2*, 7.

(33) Busch, J. H.; de la Vega, J. R. *J. Am. Chem. Soc.* **1977**, *99*, 2397.

(34) de la Vega, J. R. *Acc. Chem. Res.* **1982**, *15*, 185.

(35) Weil, D. A.; Dixon, D. A. *J. Am. Chem. Soc.* **1985**, *107*, 6859.

(36) Wolfe, S.; Hoz, S.; Kim, C.-K.; Yang, K. *J. Am. Chem. Soc.* **1990**, *112*, 4186.

5946 *J. Am. Chem. Soc., Vol. 113, No. 16, 1991*

Dodd et al.

Table II.[a] RRKM Values of E_{diff} for Thermoneutral Proton Transfer Reactions

reaction	efficiency[b]	$-E_w$[c]	$-E_{diff}^R$[d]	ΔE^*[e]
(13) MeO⁻ + MeOH	0.26	29.3	11.5	17.8
(14) EtO⁻ + EtOH	0.30	28.1	10.9	17.2
(15) t-BuO⁻ + t-BuOH	≥0.23	27.9	11.2	16.7

[a] Energies are given in kcal/mol. [b] These efficiencies are approximated by those of isotopically labeled reactions. The efficiency of reaction 1 is approximated by that of CH_3O^- + $^{13}CH_3OH$. The efficiency of reaction 2 is approximated by that of $CH_3CH_2O^-$ + CD_3CH_2OH. Both of these are good approximations since the isotopically labeled reactions are thermoneutral. The efficiency of reaction 3 is approximated by that of $(CH_3)_3CO^-$ + $(CD_3)_3COD$, a slightly endothermic reaction. This approximation is less good; the true efficiency of reaction 3 would presumably be slightly larger. [c] These stabilization energies were obtained from the value for MeOHOMe⁻, measured by Kebarle[42a] and Meot-Ner,[42b,c] and the relative stabilization energies of the different alcohol–alkoxide complexes measured by Bartmess.[43] [d] The difference in energy between the two transition states derived from RRKM analysis. The input parameters for the calculations are shown in Tables IV–VI. [e] The barrier height to proton transfer, obtained from $-(E_w - E_{diff})$.

V. Statistical Rate Theory Analysis

A thermoneutral proton-transfer reaction following a barrierless reaction coordinate, i.e., possessing a single minimum, is expected to have a reaction efficiency equal to 0.5. This situation is illustrated in Figure 1a, where the surface surrounding the ion-molecule complex is completely symmetric and, therefore, products or reactants are generated at equal rates. Reactions with efficiencies less than 0.5, however, have been successfully modeled using a double minimum surface, illustrated in Figure 1b. For this type of surface, two transition states exist: a loosely bound orbiting transition state and a tighter transition state at the saddle point. The reaction efficiency then depends on the ratio of the sum of states of the two transition states. These types of surfaces have been modeled using statistical theories, such as RRKM theory, to count the relative sums of states, and infer the necessary height of the energetic barrier.[37,38]

The details of RRKM theory and calculations have been described extensively elsewhere and will not be reviewed here.[39] However, it is instructive to examine the fundamental assumptions upon which the theory is based. First, as a statistical theory, it requires that the ion–molecule collision complex be sufficiently long-lived so that energy randomization occurs before reaction. A second, related assumption is that the energy randomization between the internal modes is possible; i.e., all modes are coupled together and energy flows easily between them. For large, long-lived complexes with many degrees of freedom, such as alkoxide–alcohol complexes, these assumptions are generally assumed to be accurate.

The essence of RRKM analysis is to estimate the frequencies associated with the two transition states (dissociation of the complex and proton transfer), and then to calculate the efficiency as a function of the difference in energies of these two transition states, called E_{diff}. The value of E_{diff} for which the calculated efficiency equals the experimentally measured efficiency is taken to describe the reaction surface. A negative value of E_{diff} implies that the proton-transfer transition state lies lower in energy than the dissociative transition state. If the stabilization energy of the collision complex, i.e., the well depth, E_w, is known, it is then possible to infer the barrier height for proton transfer in the complex: $\Delta E^* = -(E_w - E_{diff})$. The well depth, E_w, is defined

Table III.[a] Comparison of RRKM Values of E_{diff} and Marcus Theory Predictions of E_{diff} for Exothermic Reactions of CH_3O^- with Alcohols

alcohol	efficiency	ΔE_{rxn}°	$-E_{diff}^\circ$[b]	$-E_{diff}^R$[c]	$-E_{diff}^M$
(2) MeOH	0.26	0	11.5	11.5	11.5
(8) EtOH	0.40	-3.1	11.5	11.9	13.0
(9) t-BuOH	0.58	-5.9	11.5	13.1	14.3
(10) CF_3CH_2OH	0.85	-14.8	11.5	17.8	18.1

[a] Energies are given in kcal/mol. [b] The "intrinsic" E_{diff}s for all the reactions are taken to be the E_{diff}^R calculated by RRKM theory for the thermoneutral exchange reaction, MeO⁻ + MeOH. This approximation is believed to be good based on the insensitivity of E_{diff}^R to the nature of the alcohol and alkoxide, as shown in Table II. [c] These values of E_{diff} are calculated by RRKM theory using the input parameters for MeO⁻ + MeOH, given in Tables IV–VI, and plotting E_{diff} versus reaction efficiency.

as a negative number if the collision complex lies below the separated reactants and products, the general case for fast gas-phase ion–molecule reactions.

The results of simple RRKM model calculations on the three thermoneutral proton-transfer reactions, methoxide + methanol, ethoxide + ethanol, and tert-butoxide + tert-butyl alcohol, reactions 13, 14, and 15, respectively, are shown in Table II. The relevant input parameters, i.e., the frequencies of the two transition states, used in these calculations are listed in Tables IV–VI.[26b,40,41] The reaction efficiencies of reactions 13 and 14 are approximated by the efficiencies of thermoneutral reactions, (2) and (5), respectively, shown in Table I. The efficiency of reaction 15, t-BuO⁻ + t-BuOH, is approximated by that of the slightly endothermic reaction, t-BuO⁻ + C_4D_9OD (reaction 7, shown in Table I). The stabilization energy, E_w, of MeOHOMe⁻ has been measured to be 29 kcal/mol.[42] The stabilization energies of EtOHOEt⁻ and t-BuOHO-t-Bu⁻ were extracted from the MeOHOMe⁻ stabilization energy and the differences in energy between EtOHOEt⁻, t-BuOHO-t-Bu⁻, and MeOHOMe⁻, measured by Bartmess and co-workers.[43]

As can be seen in Table II, the values of E_{diff} derived from the RRKM calculations are small compared to the well depth. The corresponding barrier heights, therefore, are huge: ca. 17 kcal/mol in each case. These results clearly conflict with the relatively smooth surfaces calculated by the quantum theoreticians, discussed above. In addition, there is no other experimental support for such large barriers for simple proton-transfer reactions.

The reactions of CH_3O^- with a series of alcohols, $^{13}CH_3OH$, EtOH, t-BuOH, and CF_3CH_2OH (reactions 2, 8, 9, and 10, respectively), show a trend of slowly increasing reaction efficiency with increasing exothermicity. This slow progression is consistent with the presence of a large barrier that is gradually lowered by increasing exothermicity. The barrier heights for this series of reactions can be approximated using the input parameters for the methoxide/methanol system and calculating E_{diff} as a function of reaction efficiency. These results are shown in Table III. As expected, when the reactions become more exothermic, the difference in energy between the two transition states becomes larger, thus lowering the proton-transfer barrier.

The relationship between the reaction exothermicity and the putative E_{diff}, approximated by RRKM analysis, can be compared to Marcus theory predictions, using the equation:

$$E_{diff}^M = E^\circ{}_{diff} + \frac{\Delta E^\circ{}_{rxn}}{2} + \frac{(\Delta E^\circ{}_{rxn})^2}{16(E^\circ{}_{diff} - E_w)} \quad (4)$$

where $\Delta E^\circ{}_{rxn}$ is the reaction exothermicity, $E^\circ{}_{diff}$ is the "intrinsic"

(37) (a) Olmstead, W. N.; Brauman, J. I. *J. Am. Chem. Soc.* **1977**, *99*, 4219. (b) Olmstead, W. N.; Brauman, J. I. *J. Am. Chem. Soc.* **1979**, *101*, 3715. (c) Asubiogo, O. I.; Brauman, J. I. *J. Am. Chem. Soc.* **1979**, *101*, 3715. (d) Pellerite, M. J.; Brauman, J. I. *J. Am. Chem. Soc.* **1980**, *102*, 5993. (e) Caldwell, G.; Magnera, T. F.; Kebarle, P. *J. Am. Chem. Soc.* **1984**, *106*, 959.
(38) Chesnavich, W. J.; Bowers, M. T. In *Gas Phase Ion Chemistry*; Bowers, M. T., Ed.; Academic Press: New York, 1976; Vol. 1.
(39) (a) Forst, W. *Theory of Unimolecular Reactions*; Academic Press: New York, 1973. (b) Robinson, P. J.; Holbrook, K. A. *Unimolecular Reactions*; Interscience: London, 1972.

(40) (a) Perchard, J.-P.; Josien, M.-L. *J. Chim. Phys.* **1968**, *65*, 1834, 1856. (b) Barnes, A. J.; Hallam, H. E. *Trans. Faraday Soc.* **1970**, *66*, 1932.
(41) Korppi-Tommola, J. *Spectrochim. Acta* **1978**, *34A*, 1077.
(42) (a) Paul, G. J. C.; Kebarle, P. *J. Phys. Chem.* **1990**, *94*, 5184. (b) Meot-Ner, M.; Sieck, L. W. *J. Phys. Chem.* **1986**, *90*, 6687. (c) Meot-Ner, M.; Sieck, L. W. *J. Am. Chem. Soc.* **1986**, *108*, 7525.
(43) Caldwell, G.; Rozeboom, M. D.; Kiplinger, J. P.; Bartmess, J. E. *J. Am. Chem. Soc.* **1984**, *106*, 4660.

E_{diff} in the absence of any thermodynamic driving force, and E_{diff}^M is the energy difference calculated by Marcus theory.[44] This modified Marcus equation has the advantage of being less sensitive to the well depth of the complex, E_w, and is directly comparable to the results of RRKM calculations.[44b] Using the RRKM E_{diff}^R for the thermoneutral methoxide–methanol exchange as the "intrinsic" E°_{diff} and a constant value of $E_w = 29$ kcal/mol, the Marcus theory E_{diff}^M can be calculated for reactions 2, 8, 9, and 10. The predicted values of E_{diff}^M, Table III, are in reasonable quantitative agreement with the difference in energies between the two transition states calculated from RRKM theory, E_{diff}^R. The relationship between the reaction exothermicity and the RRKM and Marcus derived E_{diff}'s is shown in Figure 2. The line has been calculated using eq 4; the points are the derived RRKM values, E_{diff}^R.

In conclusion, given only an "intrinsic" E°_{diff} based on the experimental reaction efficiency of MeO⁻ + MeOH and the reaction exothermicity, Marcus theory is able to predict the experimental behavior of exothermic reactions quite well. This slowly increasing reaction efficiency with increasing reaction exothermicity is consistent with the large barriers calculated for the thermoneutral reactions. As discussed above, however, these results are inconsistent with the results of quantum calculations.

VI. Discussion

RRKM analysis of these simple proton-transfer systems thus presents a neat, internally consistent picture of double minimum potential wells, with sizable barriers to proton transfer. This result, however, directly conflicts with the quantum calculations described in section IV, which suggest essentially flat, barrierless, potential wells.

In support of the quantum calculations are experimental measurements of the isotope fractionation factors for the proton-bound dimers of ethoxide[45] and methoxide[35] anions. These experiments, based on an equilibrium measurement of eq 5 in the

$$\text{MeOHOMe}^- + \text{MeOD} \rightarrow \text{MeODOMe}^- + \text{MeOH} \quad (5)$$

case of methoxide–methanol, provide information on the partitioning of the proton and deuteron between the dimer and the monomer. The low reported value of $K_5 = 0.31$, which after correcting for the fractionation factor of MeOH yields a methoxide–methanol fractionation factor of 0.33, is consistent with the motion of the proton in a potential with little or no barrier.[46] A low value of K_5 implies that the zero-point energy of the alcohol–alkoxide complex is relatively similar to that of the alcohol monomer. Subsequent larger equilibrium measurements, however ($K_5 = 0.45$ by Barlow, Dang, and Bierbaum,[9] and $K_5 = 0.60$ by McMahon and co-workers,[47] which yield dimer fractionation factors of 0.48 and 0.64, respectively), make this argument less compelling.

A possible explanation for the discrepancy between the measured reaction efficiencies and the results of quantum calculations, as well as the fractionation factor measurements mentioned above, is that some vibrational modes of the system are not coupled together, and therefore energy is not randomized within the lifetime of the complex. In this case, traditional RRKM analysis would not accurately model the experimental results, since the fundamental assumption of energy randomization is violated. This type of nonstatistical behavior for alkoxide–alcohol complexes would be surprising; the complexes are strongly bound[42,43] and possess many internal degrees of freedom. In addition, high-pressure experiments show collisional quenching of these com-

Table IV. Input Parameters for RRKM Calculations for Methoxide + Methanol

orbiting transition state (CH₃O⁻···HOCH₃)			proton-transfer transition state (CH₃O·H·OCH₃)⁻		
ν_i (cm⁻¹)[a]		I_i (amu·Å), σ_i[b]	ν_i (cm⁻¹)[a,c]		I_i (amu·Å), σ_i[b]
3681	1477		3000	1455	
3000	1455	1.83, 1(1)	3000	1455	3.17, 3(1)
3000	1455	18.66, 3(2)	2960	1345	3.17, 3(1)
2960	1345	20.98, 1(2)	2960	1165	
2960	1165		2844	1165	
2844	1165		2844	1060	
2844	1060		1477	1060	
1477	1060		1477	1033	
1477	1033		1477	1033	
1477	1033		1477	300	
	250			300	
				300	
				300	
				300	

$$I_{orb(1)}/I_{PT} = 1.84; \quad I_{orb(1)}/I_{orb(2)} = 1.00$$

[a] Reference 26b, p 63. Frequencies for CH₃O⁻ were taken from those of CH₃OH. [b] Degeneracy is in parentheses. [c] Five low-frequency oscillators and a methyl rotor are created by the locking up of the two two-dimensional rotors and by the disappearance of the 250-cm⁻¹ torsional oscillation in the orbiting TS. The OH stretch becomes the reaction coordinate.

plexes, confirming that at least some of the reaction intermediates are relatively long-lived.[9,48]

Another possible resolution of this discrepancy is that the constraint of conservation of angular momentum forces the system away from its optimum geometry, creating an effective barrier on the potential energy surface. In this case, the static quantum calculations, which map a minimum energy path assuming zero angular momentum, would not adequately describe the experimental situation which involves the measurement of an ensemble-averaged quantity. The reaction system could still be statistical, and thus a more complete, RRKM-type analysis could be used to model it. However, such an analysis would explicitly include an account of angular momentum and its effects on the dynamics of the system. As mentioned in section IV, small geometry distortions in the proton-transfer complex lead to large increases in the barrier height, suggesting that the proton-transfer reaction rate would be sensitive to these effects. Our attempts to calculate the effective rotational barrier for a thermal distribution of angular momenta, using Langevin analysis, however, suggest that this effect alone cannot account for the observed decrease in reaction rates.[49]

A third, and more likely, explanation is that there are multiple transition states on the surface[3] and that the slow rates observed follow from these, rather than a simple enthalpic barrier. Quasi-classical trajectory calculations for proton-transfer on a very simple surface (diatomic neutral + atomic anion) with a 30-kcal/mol well depth and no barriers show efficiencies less than 50%. For these systems, some of the encounter complexes never enter the well; depending on the translational energy, the impact parameter, and the angular momentum of the neutral, the reactants simply redissociate.[50] One possible origin of this effect is that the locking of the rotor causes a decrease in the reaction flux to the well. Alternative language may describe this in other ways. We are not yet certain of the fully correct physical description. Although the trajectory calculations were carried out on a very simple, low-dimensional model, however, there is beginning to be a convincing case that reactions on such barrierless surfaces can indeed be slightly slowed, so that a simple application of RRKM theory in the way we have described is not the appropriate way to handle such kinetic problems. We expect that whatever the specific origin of the effect is, it has some sensitivity to the exothermicity of the reaction, so that as the reaction becomes more favorable, the probability of entering the well also increases.

(44) (a) Cohen, A. O.; Marcus, R. A. *J. Phys. Chem.* **1968**, *72*, 4249. (b) Dodd, J. A.; Brauman, J. I. *J. Phys. Chem.* **1986**, *90*, 3559. (c) Dodd, J. A.; Brauman, J. I. *J. Am. Chem. Soc.* **1984**, *106*, 5356.

(45) Ellenberger, M. R.; Farneth, W. E.; Dixon, D. A. *J. Phys. Chem.* **1981**, *85*, 4.

(46) (a) Kreevoy, M. M.; Liang, T. M. *J. Am. Chem. Soc.* **1980**, *102*, 3315. (b) Gold, V.; Grist, S. *J. Chem. Soc. B* **1971**, 1665.

(47) As quoted in ref 9: Szulejko, J. E.; Wilkinson, F. E.; McMahon, T. B. Presented at the 37th ASMS Conference on Mass Spectrometry and Allied Topics, May 1989.

(48) Osterheld, T. H.; Brauman, J. I. Unpublished results.

(49) Lim, K. F.; Brauman, J. I. *Chem. Phys. Lett.* **1991**, *177*, 326.

(50) Lim, K. F.; Brauman, J. I. *J. Chem. Phys.* **1991**, *94*, 7164.

Table V. Input Parameter for RRKM Calculations for Ethoxide + Ethanol

orbiting transition state ($CH_3CH_2O^-\cdots HOCH_2CD_3$)			proton-transfer transition state ($CH_3CH_2O\cdot H\cdot OCH_2CD_3)^-$		
ν_i (cm^{-1})[a]	I_i (amu·Å), σ_i[b]		ν_i (cm^{-1})[a,c]	I_i (amu·Å), σ_i[b]	
3676	1225		3676	1225	
2989	1200	7.87, 1(1)	2989	1200	7.87, 1(1)
2989	1134	55.43, 1(2)	2989	1134	
2949	1089	60.06, 1(2)	2949	1089	
2949	1062		2949	1062	
2943	1045		2943	1045	
2904	1033		2904	1033	
2900	1024		2900	1024	
2225	925		2225	925	
2225	925		2225	925	
2115	885		2115	885	
1490	801		1490	801	
1490	756		1490	756	
1452	668		1452	668	
1452	419		1452	419	
1415	370		1415	370	
1394	243		1394	243	
1385	201		1385	201	
1339	170		1339	300	
1251			1251	300	
				300	
				300	
				170	

$$I_{orb(1)}/I_{PT} = 1.80; \ I_{orb(1)}/I_{orb(2)} = 1.00$$

[a] Reference 40. Frequencies for EtO$^-$ were taken from those of EtOH. [b] Degeneracy is in parentheses. [c] Four low-frequency oscillators are created by the locking up of the two two-dimensional rotors. The OH stretch becomes the reaction coordinate.

VII. Conclusions

We report that proton-transfer reactions between alcohols and simple alkoxide anions are measurably slowed relative to the collision rate. Both quantum calculations and fractionation factor measurements argue against the presence of any large enthalpic
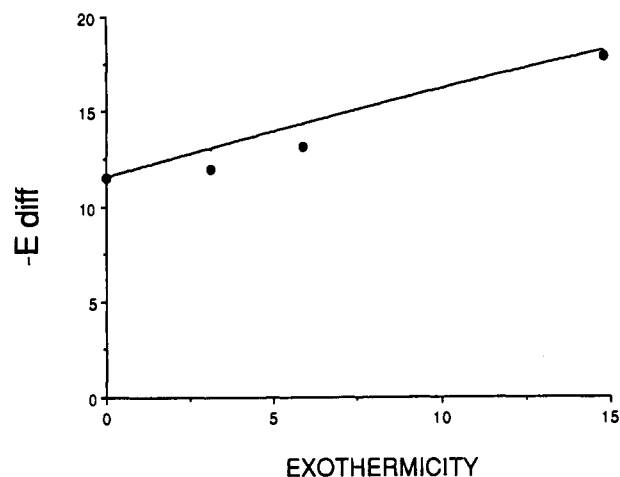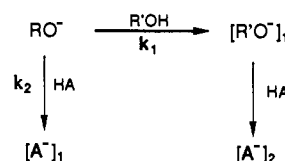

Figure 2. Plot of reaction exothermicity versus the RRKM values of E^A_{diff} (circles) and E^M_{diff} derived from Marcus theory assuming an "intrinsic" $E°_{diff}$ of −9.5 kcal/mol (line).

Scheme II

barrier on the minimum energy path of the potential surface. Langevin analysis of the effective proton-transfer barrier induced by the constraint of conservation of angular momentum suggests that this effect cannot account for the magnitude of the observed rate decreases. Quasi-classical trajectory simulations of a simplified model proton-exchange reaction indicate that the reaction efficiency can be less than 50%, even for a barrierless potential
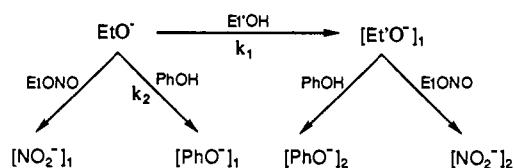
Table VI. Input Parameters for RRKM Calculations for *tert*-Butoxide + *tert*-Butyl Alcohol

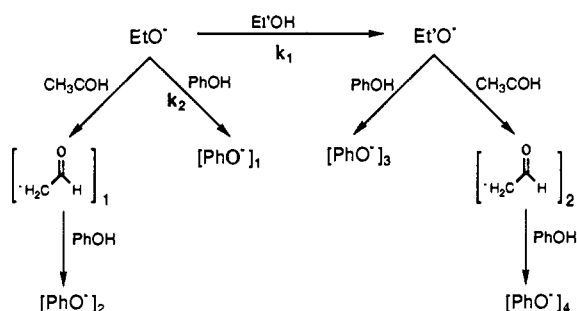| orbiting transition state (($CH_3)_3CO^-\cdots HOC(CH_3)_3$)				proton-transfer transition state (($CH_3)_3CO\cdot H\cdot OC(CH_3)_3)^-$			
ν_i (cm^{-1})[a]		I_i (amu·Å), σ_i[b]		ν_i (cm^{-1})[a,c]		I_i (amu·Å), σ_i[b]	
2943	1469	813		2943	1469	813	
2908	1373	735	0.43, 1(1)	2908	1373	735	0.43, 1(1)
2918	1373	729	136.5, 1(2)	2918	1373	729	
2988	1214	729	108.2, 1(2)	2988	1214	729	
2988	1214	814		2988	1214	814	
2973	1270	814		2973	1270	814	
2973	1140	746		2973	1140	746	
2876	915	669		2876	915	669	
2876	1027	456		2876	1027	456	
2678	1013	456		2678	1013	456	
2155	1167	396		2155	1167	396	
2133	1167	396		2133	1167	396	
2143	1049	418		2143	1049	418	
2240	1085	349		2240	1085	349	
2240	1085	348		2240	1085	348	
2230	1062	348		2230	1062	348	
2230	1062	294		2230	1062	294	
2067	1059	294		2067	1059	294	
2067	1059	270		2067	1059	270	
1464	1054	270		1464	1054	270	
1372	1054	270		1372	1054	300	
1450	1013	192		1450	1013	300	
1477	921	192		1477	921	300	
1477	921	192		1477	921	300	
1469	893	167		1469	893	270	
						192	
						192	
						192	
						167	

$$I_{orb(1)}/I_{PT} = 3.26; \ I_{orb(1)}/I_{orb(2)} = 1.00$$

[a] Reference 41. Frequencies for *t*-BuO$^-$ were taken from those of *t*-BuOH. [b] Degeneracy is in parentheses. [c] Four low-frequency oscillators are created by the locking up of the two two-dimensional rotors. The OH stretch becomes the reaction coordinate.
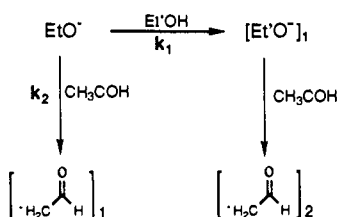
Scheme III

$$EtO^- \xrightarrow[k_1]{Et'OH} [Et'O^-]_1$$

EtONO / PhOH k_2 / PhOH / EtONO

$[NO_2^-]_1$ $[PhO^-]_1$ $[PhO^-]_2$ $[NO_2^-]_2$

Scheme IV

$$EtO^- \xrightarrow[k_1]{Et'OH} Et'O^-$$

CH$_3$COH / PhOH k_2 / PhOH / CH$_3$COH

$\left[\cdot H_2C\overset{O}{\underset{}{\diagdown}}H \right]_1$ $[PhO^-]_1$ $[PhO^-]_3$ $\left[\cdot H_2C\overset{O}{\underset{}{\diagdown}}H \right]_2$

PhOH   PhOH

$[PhO^-]_2$ $[PhO^-]_4$

Scheme V

$$EtO^- \xrightarrow[k_1]{Et'OH} [Et'O^-]_1$$

k_2 | CH$_3$COH   CH$_3$COH

$\left[\cdot H_2C\overset{O}{\underset{}{\diagdown}}H \right]_1$ $\left[\cdot H_2C\overset{O}{\underset{}{\diagdown}}H \right]_2$

surface. We thus suggest that the slow measured reaction rates could be due in part to the presence of multiple transition states along the association pathway which hinder formation of the reaction intermediate necessary to proton transfer.

Appendix A. Derivations for the Competitive Rate Measurements

For a proton-transfer reaction involving no side reaction, the competition technique processes are illustrated in Scheme I. The desired quantity is the ratio of the reaction rate to form $R'O^-$ over the reaction rate with a reference acid, HA. This quantity k_1/k_2 is equal to the ratio of their primary reaction yields, $[R'O^-]_1/[A^-]_1$. Since $R'O^-$ subsequently reacts to form A^-, the primary yields must be extracted. The various reaction processes are shown in Scheme II, where the subscript "1" refers to the primary yield and "2" refers to the secondary yield. The experimental measurements are the total A^- signal, $[A^-]_T = [A^-]_1 + [A^-]_2$, and the A^- signal when $R'O^-$ is continuously ejected from the cell, $[A^-]_e = [A^-]_1$, where the subscript "T" refers to the total intensity

observed in the absence of any ion ejections, and "e" refers to the quantity observed in the presence of continuous ejection of $R'O^-$. Thus the desired ratio, $[R'O^-]_1/[A^-]_1$, simply equals $([A^-]_T - [A^-]_e)/[A^-]_e$.

Rate measurements involving generation of ethoxide from ethyl nitrite are complicated by the formation of NO_2^-, from reaction of EtO^- with EtONO to form diethyl ether as the neutral product. NO_2^- is a weak base and does not abstract a proton from phenol, the reference acid used. The reaction processes involved are shown in Scheme III. As in the simpler case shown above, the desired quantity is k_1/k_2, which equals $[Et'O^-]_1/[PhO^-]_1$.

The experimentally observed quantities are

$$[PhO^-]_T = [PhO^-]_1 + [PhO^-]_2$$

$$[NO_2^-]_T = [NO_2^-]_1 + [NO_2^-]_2$$

$$[PhO^-]_e = [PhO^-]_1$$

$$[NO_2^-]_e = [NO_2^-]_1$$

where the subscripts are defined as above. Simple algebra is then used to extract the desired relationship:

$$\frac{[Et'O^-]_1}{[PhO^-]_1} = \frac{([PhO^-]_T - [PhO^-]_e) + ([NO_2^-]_T - [NO_2^-]_e)}{[PhO^-]_e} \quad (6)$$

Ethoxide ion can also be generated from diethyl peroxide. Acetaldehyde enolate anion is also generated from a side reaction of ethoxide with acetaldehyde formed by pyrolysis of the neutral on the filament. Acetaldehyde is a weaker acid than phenol (the reference acid used), and thus its anion subsequently abstracts a proton from phenol. These reaction processes are illustrated in Scheme IV, where the subscripts "3" and "4" refer to the yields of these reactions, respectively, and the other subscripts are defined as above.

In order to determine k_1/k_2, it is first necessary to examine the system in the absence of phenol. This simplified scheme is shown in Scheme V. The measured experimental quantities are:

$$[C_2H_3O^-]_T = [C_2H_3O^-]_1 + [C_2H_3O^-]_2$$

$$[C_2H_3O^-]_e = [C_2H_3O^-]_1$$

where the subscripts are defined as above. Phenol is then introduced and the process is repeated. The experimentally measured quantities are:

$$[PhO^-]_T = [PhO^-]_1 + [PhO^-]_2 + [PhO^-]_3 + [PhO^-]_4$$

$$[PhO^-]_e = [PhO^-]_1 + [PhO^-]_2$$

Again, using algebra, the four experimental quantities can be manipulated to yield the equation:

$$\frac{[Et'O^-]_1}{[PhO^-]_1} = \frac{[PhO^-]_T - [PhO^-]_e}{[PhO^-]_e - [C_2H_3O^-]_e} \quad (7)$$